Semi-Automatic Delineation of the Spino-Laminar Junction Curve on Lateral X-ray Radiographs of the Cervical Spine

Benjamin Narang[a], Michael Phillips[b], Karen Knapp[c],
Andy Appelboam[d], Adam Reuben[d], Greg Slabaugh[*b]

[a]ENSTA ParisTech, Boulevard des Marchaux, Palaiseau, France;
[b]City University London, Northampton Square, London, UK;
[c]University of Exeter, Devon, UK;
[d]Royal Devon and Exeter Hospital, Barrack Road, Devon, UK

ABSTRACT

Assessment of the cervical spine using x-ray radiography is an important task when providing emergency room care to trauma patients suspected of a cervical spine injury. In routine clinical practice, a physician will inspect the alignment of the cervical spine vertebrae by mentally tracing three alignment curves along the anterior and posterior sides of the cervical vertebral bodies, as well as one along the spinolaminar junction. In this paper, we propose an algorithm to semi-automatically delineate the spinolaminar junction curve, given a single reference point and the corners of each vertebral body. From the reference point, our method extracts a region of interest, and performs template matching using normalized cross-correlation to find matching regions along the spinolaminar junction. Matching points are then fit to a third order spline, producing an interpolating curve. Experimental results demonstrate promising results, on average producing a modified Hausdorff distance of 1.8 mm, validated on a dataset consisting of 29 patients including those with degenerative change, retrolisthesis, and fracture.

Keywords: Cervical spine injuries, Normalized cross-correlation, Pattern recognition, Spinolaminar junction

1. INTRODUCTION

Cervical spine injuries (CSIs) occur in approximately 4.3% of all trauma patients.[1] These injuries typically result from high energy impact, involving automobile accidents (44%), falls (22%), dives into shallow water (15%) and other causes.[2] CSI can also occur with more minor injuries in elderly patients and in those with pre-existing bone abnormalities.

Evaluation of cervical spine radiographs is often a pressing diagnostic challenge for emergency physicians, as up to 20% of CSI patients suffer extension of their injuries due to delayed or missed diagnosis,[3] which can have severe consequences to the patient. Often three radiographs are taken from lateral, odontoid, and anteroposterior views.[4] The lateral image provides a side view, ideally of all seven cervical vertebrae (labeled C1 to C7), and is considered to be the most diagnostic view for assessing the alignment of the cervical spine vertebrae; an example lateral radiograph of the cervical spine is shown in Figure 1(a). The emergency physician examines the alignment of the cervical spine by mentally tracing curves along the spine, along the anterior vertebral body, posterior vertebral body, and spino-laminar junction, the latter of which follows the interior edge of the spinous processes. These three curves have been visualized in Figure 1(c), as purple, red, and blue curves, respectively.

In this paper, we present a semi-automatic approach to delineate the spinolaminar junction. The input to the algorithm is a set of vertebral body corners, and a user-supplied click point on the spinolaminar junction. An example is shown in Figure 1(b), where the click point is rendered as a blue circle, and the vertebral body corners are rendered as yellow "x"s, which can be obtained from a vertebral body segmentation algorithm, or provided manually. Vertebral body segmentation is not discussed in detail in this paper as it has been addressed in previous literature.[5,6] For each vertebra, we extract a 2D region of interest and perform template matching using normalized cross-correlation to find a matching point on the spinolaminar junction. The detected spinolaminar

*gregory.slabaugh.1@city.ac.uk; telephone: +44 (0)207 040 8416

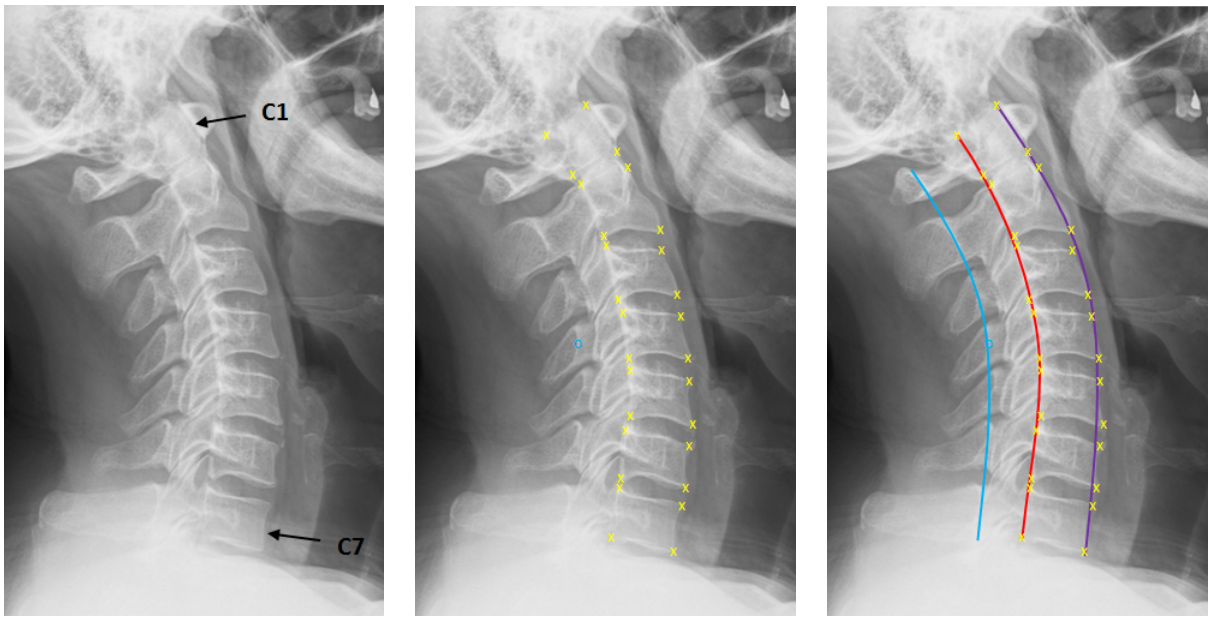

(a) (b) (c)

Figure 1. In (a), we show a cervical spine radiograph, which shows all seven cervical vertebrae, starting with C1 at the top, down to C7. The input to our approach is a set of vertebral body corner points, rendered as yellow "x"s in (b), along with a click point on the spinolaminar junction, rendered as a blue circle in (b). The approach detects other points on the spinolaminar junction, and fits a spline. A mock-up appears in (c), rendering the spinolaminar curve as blue. For completeness, we also show the posterior and anterior curves as red and purple, respectively; however, the purpose of this paper is to compute the blue curve from the inputs shown in (b).

junction points are fit to a third order spline, which is overlaid on the image to provide support to the physician reading the image. Experimental results demonstrate promising performance of the proposed method, with a good agreement of the detected curves with those produced manually by an expert radiographer.

1.1 Related work

Given the clinical important of spinal imaging, there has been considerable work on computational methods to analyze images of the spine. A fundamental problem is segmentation of the vertebrae, and research has been conducted in segmentation of cervical spine radiographs,[5,6] typically using active shape models.[7] Other work investigates spinal segmentation using related modalities like computed tomography[8,9] and digitally reconstructed radiographs.[10]

Given a segmentation, automated radiographic assessment of vertebral morphometry[11,12] detects abnormalities from the extracted vertebral shapes, and can detect injuries such as biconcave, wedge, and crush fractures. The type and severity of a fracture can be classified using the Genant semi-quantitative criteria.[13] While there is some interest in the literature in computer-aided detection (CAD) of fractures on cervical spine radiographs,[14,15] there is limited research on this topic, possibly due to the lack of available data. Many researchers working in the field use the NHANES II[16] dataset, however, this dataset may be inappropriate for developing image analysis approaches for cervical spine injuries, as the data was not collected from emergency room patients.

Closest to the proposed work is Larhmam et al.,[15] who describe method to segment the cervical spine vertebrae and detect alignment curves using a mean vertebral shape, generalized Hough transform, and k-means clustering approach. From the detected vertebrae, the three alignment curves, including the spinolaminar junction curve, are computing using quadratic splines. While[15] demonstrates the possibility of alignment curve computation, the paper provides no quantitative results on the accuracy of the detected curves. Furthermore, the approach taken in[15] only provides segmentations and alignment curves between the C3 and C7 vertebrae, as the C1 and C2 vertebrae are unmodelled. In contrast, our approach computes the spinolaminar junction curve over the entire length of the cervical spine. In addition, this paper provides quantitative results in terms of Hausdorff distance,

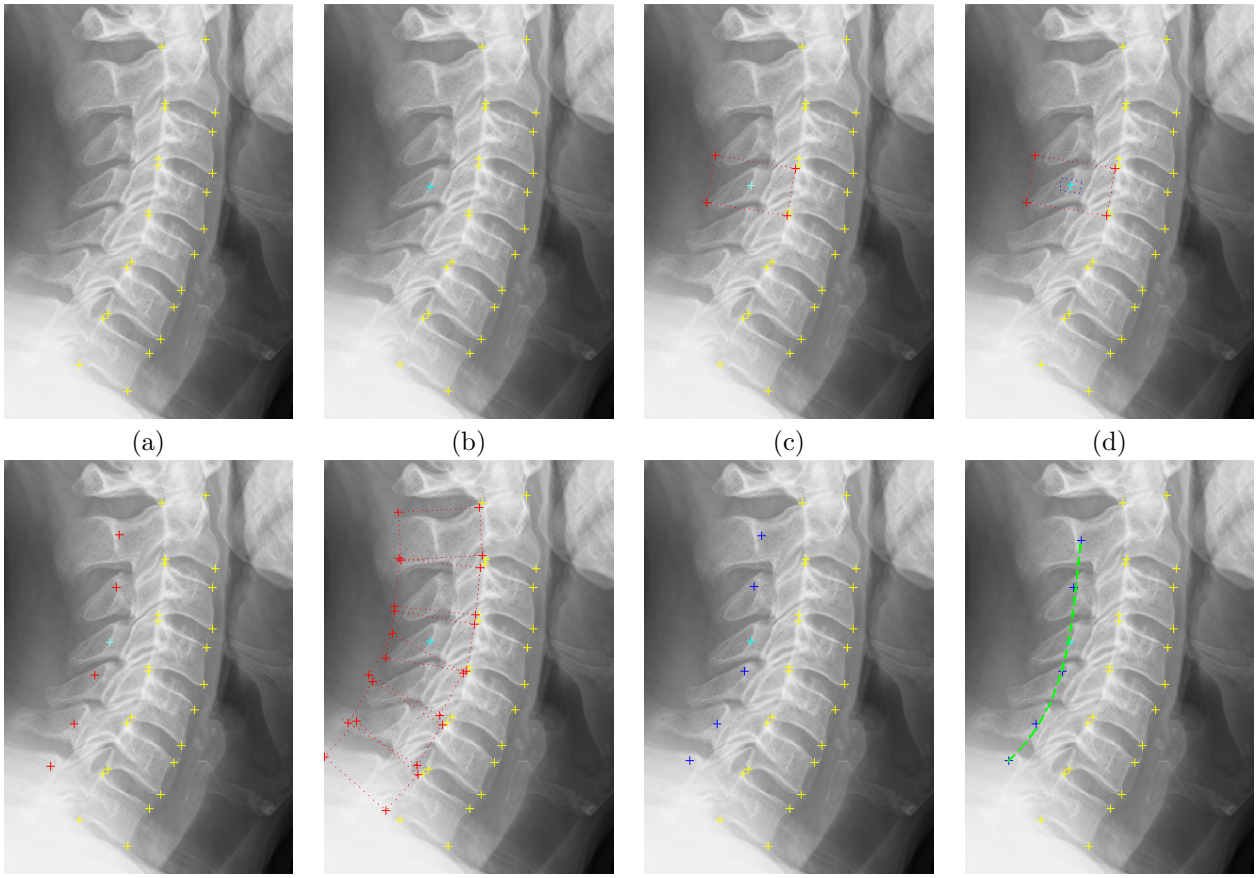

Figure 2. Steps of the algorithm. Given a set of corner points (a, yellow points) and a reference point on the spinolaminar junction (b, cyan point), we define a ROI (c, red box) around the click point and extract a template (d, blue box). For each vertebra, we extract a ROI by finding a center point (e, red points) and compute a box aligned to the vertebral body (f, red boxes). We run the template matching algorithm within each ROI to find a best match (g, blue points). We then fit a cubic spline to the detected points (h, green curve).

demonstrating the numerical accuracy of the detected curves relative to to delineations provided by an expert radiographer.

2. METHODOLOGY

The steps of the approach are outlined in Figure 2 and described in more detail below.

2.1 Region of interest and template extraction

First, a 2D Gaussian filter (zero mean, with variance $\sigma = 0.5$ pixels) is applied to the image to reduce noise. Next, the user supplies a point on the spinolaminar junction, as shown in Figure 2(b). Around the click point, we extract a region of interest (ROI) with the same orientation of the corresponding vertebrae, shown in Figure 2(c). This orientation is based on the vertebral body shape, and is given by the direction $\mathbf{d}$, which in most cases is the normalized mean of two normalized direction vectors, $\hat{\mathbf{d}}_1$, formed from the line connecting the top and bottom posterior corners, and $\hat{\mathbf{d}}_2$, formed from the line connecting the bottom posterior corner of the vertebral body above and the top posterior corner of the vertebra beneath. If the vertebra has either no vertebra above and below, then just $\hat{\mathbf{d}}_1$ is used. A rotation matrix is formed so that the extracted ROI will be axis-aligned. The width and the height of the ROI are set automatically based on the vertebral body size, as $[a_i w_i,\ b_i h_i]$, where

w_i, h_i is the width and height respectively, of the ith vertebral body, and a_i and b_i are scaling terms. We set $[a_i, b_i] = [2, 1]$ for the C1 and C2 vertebrae and $[5/4, 3/4]$ for the remaining vertebrae. We also compute the distance L, between the user click point and the center of its corresponding vertebral body.

The template is extracted around the click point, by extracting the central region (1/4 of the width and height) of the ROI containing the click point. An example template appears in Figure 2(d). For the remaining vertebrae, we extract a ROI using a similar approach as described above. The ROI is positioned so that its center is a distance L from the center of its corresponding vertebral body; examples are shown in Figure 2(f).

2.2 Template matching and curve fitting

Next, our method performs template matching of the template in each ROI, using two-dimensional normalized cross-correlation[17] (NCC) to find a best-matching point for each vertebra. Given a $N \times M$ template T, a ROI R, that overlaps with the template as R_{xy}, the normalized cross-correlation computed at a point (x, y) is given by

$$\mathrm{NCC}(x,y) = \frac{1}{NM} \sum_{i=1}^{N} \sum_{j=1}^{M} \frac{\left(R_{xy}(i,j) - \overline{R_{xy}}\right)\left(T(i,j) - \overline{T}\right)}{\sigma_{R_{xy}} \sigma_T}, \text{with} \tag{1}$$

$$\overline{g} = \frac{1}{NM} \sum_{i=1}^{n} \sum_{j=1}^{m} g(i,j), \qquad \text{and} \qquad \sigma_g = \sqrt{\frac{1}{NM} \sum_{i=1}^{N} \sum_{j=1}^{M} \left(g(i,j) - \overline{g}\right)^2} \tag{2}$$

where g is a generic variable representing either T or R_{xy} in Equation 1. The point (x, y) with the highest NCC is selected as the matching point for the ROI. Using least squares, we fit the detected points to a third-order spline. As our spinolaminar junction curve goes from the C1 to C7 vertebrae, a third-order spline is preferred, unlike,[15] which employs a second-order spline between the C3 and C7 vertebrae. The third-order spline has sufficient flexibility to model the patient geometry, and its choice is motivated by the literature.[18]

3. RESULTS

Our dataset consists of 29 patients (17 female, 12 male), with ages ranging between 30 and 94 (mean = 58.5, std dev = 18.3). Our dataset includes two patients with fractures, three with retrolisthesis, and 12 with degenerative change. For each patient, an expert radiographer manually traced points on the spinolaminar junction and a third order spline was fit, establishing the ground truth for the spinolaminar junction curve.

We applied the proposed technique to the 29 patient images, and Figure 3 shows results for eight patients, and is a representative result of the data set. In each image, given the click point (rendered as a cyan circle), the algorithm produces the green curve. The cyan curve is a rendering of the ground truth. Generally the algorithm produces results that are in good correspondence with the ground truth curve, and results (a) through (e) show a close match. Results in (f) and (g) show that sometimes the spinolaminar junction point for the C1 vertebra is misdetected, and the resulting curve veers from the ground truth. The result in (h) shows the worst result, where the NCC fails to detect points on the spinolaminar junction.

We performed a quantitative analysis comparing ground truth curve to the one estimated by our proposed method. For this, we compute the modified Hausdorff distance (MHD), which measures the average maximum distance between the closest points on the two curves for their common region of overlap. The results are presented in Table 1. The algorithm produced a mean MHD of 1.8 mm, indicating a good overall performance. MHD results are provided in the caption for the eight results in Figure 3. Also in the caption are cues as to whether the patient had degenerative change (DG) and/or retrolisthesis (RL).

For comparison, we ran a variant of the approach that uses the sum of squared differences (SSD) instead of the NCC. These results are also presented in Table 1, and indicate the NCC is superior, which is explained by the intra-patient variability in the appearance of the spinolaminar junction, which the NCC handles better. We also performed a sensitivity analysis, to see how dependent the results are on the user click point. We displaced the click point along a random 2D direction by a radius of $r = [0, 0.7, 1.4, 2.1, 2.9]$ mm. The average MHD was found to be quite stable as MHD = $[1.8, 1.9, 2.0, 2.2, 2.3]$ mm respectively.

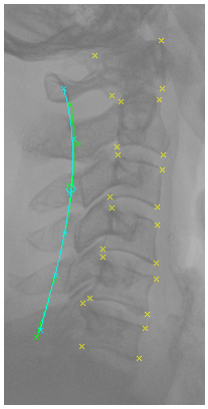

(a)
DG; MHD = 0.49 mm

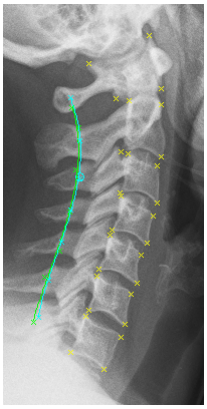

(b)
normal; MHD = 0.81 mm

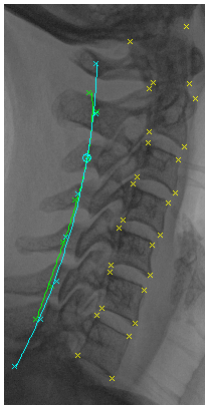

(c)
normal; MHD = 0.88 mm

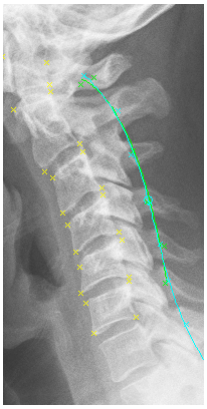

(d)
DG; MHD = 0.69 mm

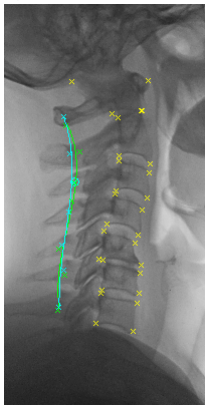

(e)
DG; MHD = 1.04 mm

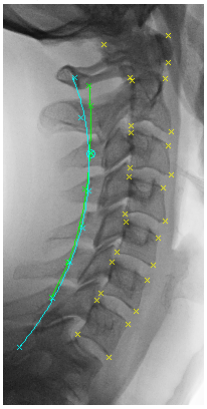

(f)
DG; MHD = 1.50 mm

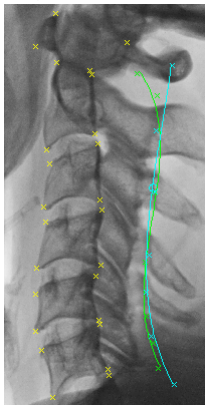

(g)
RL, DG; MHD = 2.10 mm

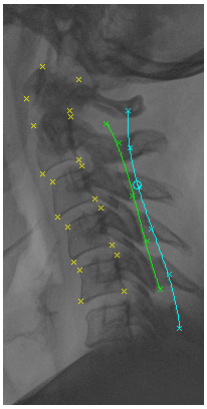

(h)
RL, DG; MHD = 4.21 mm

Figure 3. Results demonstrating the algorithm performance. See text for further details.

4. DISCUSSION AND CONCLUSION

While further experimentation is ongoing, the results presented in this paper demonstrate the promise of this method to delineate the spinolaminar junction in lateral x-ray images. A mean MHD of 1.8 mm provides good performance. Given the method's simplicity, it completes in only a few seconds after the user supplies the click point, using unoptimized Matlab code.

Despite the method's successes, there is room for improvement. Particularly sometimes the NCC returns erroneous results due to false matches. This could be addressed in a variety of ways, including more sophisticated voting strategies, for example Hough Forest,[19] or incorporating priors on the curve geometry, built using a database of ground truth spinolaminar junction curves. Another issue to be addressed in future work is automation of the user click point, so that the technique is fully automatic. While it would be possible to use active shape models that include a point on the spinolaminar junction as part of a vertebra segmentation approach as done in,[15] doing so adds complexity to the shape model. In addition, current cervical spine vertebrae segmentation approaches[5,6] that have appeared in the literature are limited to segmentation of the C3 to C7 vertebrae, given the difficulty of robustly building (and segmenting) C1 and C2 vertebrae given lack of contrast in radiographic images. While this paper assumes corners of the C1 and C2 vertebral bodies are available to build the ROIs, it may be possible to extrapolate the detected curve on C3 to C7 for ROI generation, for images where the vertebral corners are unavailable for C1 and C2. However this is left for future work.

Finally, we are interested in how alignment curves such as the spinolaminar junction curve can assist in human interpretation of the image. Overlaying the spinolaminar junction curve directly on the image may assist the clinical reader in assessing the overall alignment of this part of the spine. However degree to which the

	SSD	NCC
mean MHD	2.0 mm	**1.8** mm
min MHD	0.55 mm	**0.49** mm
max MHD	4.5 mm	**4.2** mm

Table 1. Quantitative results showing the MHD when using the SSD and NCC.

spinolaminar junction curve overlay is helpful must be established through an observer study.

ACKNOWLEDGMENTS

This work was supported by the UK Engineering and Physical Sciences Research Council grant number EP/K037641/1.

REFERENCES

[1] Benjelloun, M., Mahmoudi, S., and Lecron, F., "Computed tomography versus plain radiography to screen for cervical spine injury: A meta-analysis," *J. of Trauma* **58**(8) (2005).
[2] Platzer, P., Hauswirth, N., Jaindl, M., Chatwani, S., Vecsei, V., and Gaebler, C., "Delayed or missed diagnosis of cervical spine injuries," *Trauma* **61**(1) (2006).
[3] Davis, J. W., Phreaner, D. L., Hoyt, D. B., and Mackersie, R. C., "The etiology of missed cervical spine injuries," *Journal of Trauma-Injury Infection & Critical Care:* (March 1993).
[4] Graber, M. and Kathol, M., "Cervical spine radiographs in the trauma patient," *American Family Physician* **59**(2) (1999).
[5] Benjelloun, M., Mahmoudi, S., and Lecron, F., "A framework of vertebra segmentation using the active shape model-based approach," *International Journal of Biomedical Imaging* (2011).
[6] Xu, X., Hao, H.-W., Xu-Cheng, Y., Liu, N., and Shafin, S., "Automatic Segmentation of Cervical Vertebrae in X-ray Images," in [*Intl. Joint Conf. on Neural Networks*], (2012).
[7] Cootes, T., Taylor, C., Cooper, D., and Graham, J., "Active shape models - their training and application," *Computer Vision and Image Understanding* **61** (1995).
[8] Klinder, T., Ostermann, J., Ehm, M., Franz, A., Kneser, R., and Lorenz, C., "Automated model-based vertebra detection, identification, and segmentation in ct images," *Medical Image Analysis* **13**(3), 471 (2009).
[9] Lim, P., Bagci, U., and Bai, L., [*Computational Methods and Clinical Applications for Spine Imaging*], vol. 17 of *Lecture Notes in Comptuational Vision and Biomechanics*, ch. A Robust Segmentation Framework for Spine Trauma Diagnosis.
[10] Dong, X. and Zheng, G., "Automated Vertebra Identification from X-Ray Images," in [*Image Analysis and Recognition*], (2010).
[11] Casciaro, S. and Massoptier, L., "Automatic Vertebral Morphometry Assessment," in [*EMBC*], (2007).
[12] de Bruijne, M., Lund, M. T., Tanko, L. B., Petersen, P. C., and Nielsen, M., "Quantitative vertebral morphometry using neighbor-conditional shape models," *Medical Image Analysis* **11**(5), 503 (2007).
[13] Genant, H. K., Wu, C. Y., van Kuijk, C., and Nevitt, M. C., "Vertebral fracture assessment using a semiquantitative technique," *Journal of Bone Mineral Research* **8**(9), 1137 (1993).
[14] Aouache, M., Hussain, A., Samad, S. A., Hamzaini, A., and Ariffin, A., "Active Shape Modeling of Medical Images for Vertebral Fracture Computer Assisted Assessment System," in [*Student Conference on Research and Development*], (2007).
[15] Larhmam, M. A., Benjelloun, M., and Mahmoudi, S., "Vertebra identification using template matching modelmp and k-means clustering," *International Journal of Computer Assisted Radiology and Surgery* **9**(2), 177 (2007).
[16] Centers for Disease Control and Prevention, "Nhanes II project database," in [*http://archive.nlm.nih.gov/proj/dxpnet/nhanes/nhanes.php*],
[17] Tsai, D.-M. and Lin, C.-T., "Fast normalized cross correlation for defect detection," *Pattern Recognition Letters* **24**, 2625–2631 (November 2003).
[18] Vrtovec, T., Pernus, F., and Likar, B., "A review of methods for quantitative evaluation of spinal curvature," *European Spine Journal* **18**(5) (2009).
[19] Gall, J., Yaho, A., Razavi, N., Gool, L. V., and Lempitsky, V., "Hough forests for object detection, tracking, and action recognition," *IEEE Transactions on Pattern Analysis and Machine Intelligence* **33**(11), 2188 (2011).